CHEMISTRY OF MATERIALS

ARTICLE

pubs.acs.org/cm

Solvothermal Soft Chemical Synthesis and Characterization of Nanostructured $Ba_{1-x}(Bi_{0.5}K_{0.5})_xTiO_3$ Platelike Particles with Crystal-Axis Orientation

Xingang Kong, Dengwei Hu, Yoshie Ishikawa, Yasuhiro Tanaka, and Qi Feng*

Department of Advanced Materials Science, Faculty of Engineering, Kagawa University, 2217-20 Hayashi-cho, Takamatsu-shi, 761-0396 Japan

Supporting Information

ABSTRACT: This paper introduces a $Ba_{0.5}(Bi_{0.5}K_{0.5})_{0.5}TiO_3$ (BBKT) platelike particle constructed from cuboidlike nanocrystals which arrange in the same crystal-axis-orientation direction. This platelike particle is synthesized via a novel two-step solvothermal soft chemical process. In the first step, platelike particles of a layered titanate $H_{1.07}Ti_{1.73}O_4$ (HTO) precursor is solvothermally treated in $Ba(OH)_2$ solution to obtain platelike particles of a $BaTiO_3$−HTO (BT−HTO) nanocomposite. In the second step, the nanocomposite particles are hydrothermally treated in $BiCl_3$−KOH solution to obtain the BBKT platelike particles. The formation reaction and nanostructure of the BBKT platelike particles were characterized by X-ray diffraction (XRD), field-emission scanning electron microscopy (FE-SEM), transmission electron microscopy (TEM), selected-area electron diffraction (SAED), and energy-dispersive spectroscopy (EDS). BBKT platelike particles prepared via this method present an SAED pattern similar to the single crystal, although it is a polycrystalline particle. All the BBKT nanocrystals in each platelike BBKT particle have the same orientation to the [110]-direction. There is a definite relationship between the crystal-axis directions of the HTO precursor and the BBKT product.

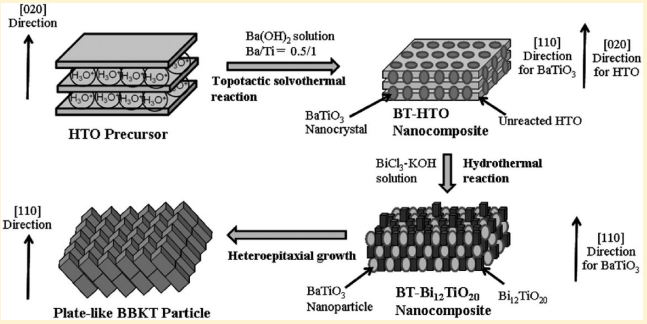

KEYWORDS: nanostructured polycrystalline particle, crystal-axis-orientation, solvothermal reaction, lead-free piezoelectric material

INTRODUCTION

The solvothermal soft chemical process is a useful and unique method for the preparation and design of functional inorganic materials.[1−3] This process typically comprises two steps: the first step is the preparation of a framework precursor with layered structure and insertion of template ions or molecules (structure-directing agents) into its interlayer space by a soft chemical reaction, and the second step is the structural transformation of the template inserted precursor into a desired structure by a solvothermal reaction. The crystal structure of the product can be controlled by the used template, and the product particle morphology is dependent on the morphology of the used precursor. This method has been utilized for the synthesis and design of metal oxides and organic−inorganic nanocomposites with controlled structure, morphology, and chemical composition.[4−6]

In the study of particle morphology control, we have prepared $BaTiO_3$ (BT) platelike particles with [110]-crystal-axis orientation via solvothermal treatment of layered titanate $H_{1.07}T_{1.73}O_4 \cdot nH_2O$ (HTO) particles with platelike morphology in a $Ba(OH)_2$ solution.[7] In the solvothermal reaction, the layered structure of HTO precursor is transformed to a BT perovskite structure by an in situ topotactic structural transformation reaction, and the particle morphology of the HTO precursor remains after the reaction. The platelike particles of BT prepared via this method are constructed from spherical nanocrystals that are arranged in the same crystal-axis orientation. Such BT platelike particles have potential applications to the fabrication of crystal-axis-oriented BT materials, such as oriented dielectric and piezoelectric materials.[8]

Recently, lead-free piezoelectric materials, such as $BaTiO_3$, $Bi_{0.5}K_{0.5}TiO_3$, $KNbO_3$, and $NaNbO_3$, have attracted considerable attention to the increasing potential application on environmental benign materials.[9−12] These lead-free piezoelectric materials, however, have a common drawback; their piezoelectric constants are much lower than that of $Pb(Zr,Ti)TiO_3$ (PZT), which is an excellent and widely used piezoelectric material; however, this material contains a large amount of lead, which is an environmental pollutant. To enhance the piezoelectricity, two types of approach have been reported. One is the application of domain engineering. The domain engineering studies suggest that the piezoelectricity of the piezoelectric ceramics can be enhanced greatly by decreasing the domain size,[13,14] and the

Received: May 30, 2011
Revised: July 20, 2011
Published: August 16, 2011

domain size can be decreased by reducing the grain size of the ceramic.[15] Another approach is use crystal-axis-oriented materials, because the piezoelectric materials show crystal-axis anisotropy. Some methods, such as templated grain growth method and reactive templated grain growth method, have been developed to fabricate the crystal-axis-oriented ceramics.[16] In these methods, the template particles with platelike or fibrous morphology are necessary, because they can be oriented easily via mechanical methods.

A [110]-axis-oriented BT ceramic has been fabricated by the templated grain growth method using the [110]-oriented BT platelike particles as the template.[8] The BT ceramic fabricated by this method exhibits a high orientation degree of 85% and a very large piezoelectric constant d_{33} value of 788 pC/N. For the practical applications as a piezoelectric material, however, the working temperature range of BT is limited by its relatively lower Curie temperature (T_c) of 120 °C and higher phase transition temperature from tetragonal phase to orthorhombic phase of ~0 °C.[17] $Bi_{0.5}K_{0.5}TiO_3$ (BKT) with a perovskite structure is another ferroelectric material with a higher T_c of 380 °C.[18] However, a dense BKT ceramic is very difficult to obtain, because of the high volatility of the potassium at high sintering temperatures.[19] To solve these problems, recently some studies have focused on $Ba_{1-x}(Bi_{0.5}K_{0.5})_xTiO_3$ (BBKT) solid solution.[20−25] Comparison with BT, not only the T_c of BBKT shifts to higher temperatures, but the phase transition from tetragonal phase to orthorhombic phase shifts to a lower temperature,[20] which expands the working temperature range of the piezoelectric material. Furthermore, the high-density BBKT ceramic can be obtained in a composition range of $x < 0.6$, and the sintering temperature become lower with increasing the x value.[20] To enhance the piezoelectricity, the oriented BBKT ceramic has been prepared via a reactive templated grain growth method, using platelike $Bi_4Ti_3O_{12}$ particles as the template.[22,23] The oriented BBKT ceramic exhibits a larger piezoelectric constant d_{33} value than that of nonoriented ceramics.

To fabricate further high-performance piezoelectric materials, the application of the domain engineering to the oriented ceramics is expected. Until now, however, it has not been achieved yet, because the fabrication of an oriented ceramic with small grain size has not been achieved. For the fabrication of the oriented ceramic with small grain size, the platelike template particle must be a nanocrystal. In the most cases, however, platelike template particles with micrometer size are used, because such particles can be oriented easily via mechanical methods in the oriented ceramic fabrication process.[26,27] Very recently, we have fabricated a [110]-oriented $Ba_{0.9}Ca_{0.1}TiO_3$ ceramic with a high orientation degree (75.8%) and small grain size (~1−2 μm), using a [110]-oriented $Ba_{0.9}Ca_{0.1}TiO_3$ platelike particle as the template.[28] This platelike template particle is constructed from the spherical nanocrystals. This result suggests that the platelike particle constructed from the nanocrystals has a great possibility for the fabrication of oriented ceramics with small grain size.

In this paper, we describe the preparation of the platelike BBKT particles by a novel two-step solvothermal soft chemical process, the formation reaction mechanism, and the characterization of the platelike particles. The platelike BBKT particle prepared via this method is constructed from cuboidlike BBKT nanocrystals, which are arranged in the same crystal-axis orientation. The platelike BBKT particle is very difficult to prepare via the normal method, because of its complex chemical composition. The success in preparing the platelike BBKT particle is a significant milestone to challenge the high performance lead-free piezoelectric materials by applying the domain engineering to the oriented ceramics.

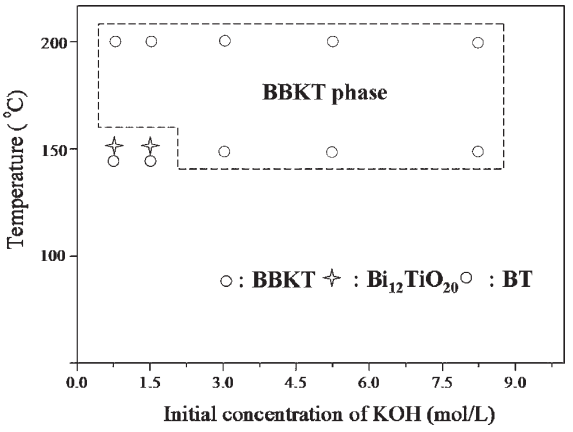

Figure 1. Phase diagram for HTO−$Ba(OH)_2$−$BiCl_3$−KOH reaction system under hydrothermal conditions.

EXPERIMENTAL SECTION

Synthesis of $Ba_{0.5}(Bi_{0.5}K_{0.5})_{0.5}TiO_3$ by One-step Hydrothermal Process. The starting material of the layered titanate $H_{1.07}Ti_{1.73}O_4 \cdot nH_2O$ (HTO) with platelike particle morphology was prepared using the method described in the literature.[29] According to the stoichiometric composition of $Ba_{0.5}(Bi_{0.5}K_{0.5})_{0.5}TiO_3$, HTO (0.094 g), $BiCl_3$, $Ba(OH)_2$, and 30 mL of a desired-concentration KOH water solution were placed in a Teflon-lined, sealed stainless-steel vessel with an inner volume of 85 mL, and then hydrothermally treated at a desired temperature for 12 h under stirring conditions. After the hydrothermal treatment, the product was filtered, washed with distilled water, and then dried at room temperature.

Synthesis of $Ba_{0.5}(Bi_{0.5}K_{0.5})_{0.5}TiO_3$ via a Two-Step Solvothermal Process. In the two-step solvothermal process for $Ba_{0.5}(Bi_{0.5}K_{0.5})_{0.5}TiO_3$, first, the $BaTiO_3$−HTO (BT-HTO) nanocomposite sample was prepared via the solvothermal treatment of HTO (0.094 g) and anhydrous $Ba(OH)_2$ (molar ratio of Ba/Ti = 0.5:1) in 30 mL of a water−ethanol mixed solvent (volume ratio = 2:28) at 150 °C for 12 h under stirring conditions. After the solvothermal treatment, evaporation was performed at 90 °C to remove the solvent. In the second step, according to the stoichiometric composition of $Ba_{0.5}(Bi_{0.5}K_{0.5})_{0.5}TiO_3$, the obtained $BaTiO_3$−HTO nanocomposite, $BiCl_3$, and 30 mL of desired concentration KOH water solution were placed in a Teflon-lined, sealed stainless-steel vessel with an inner volume of 85 mL, and then hydrothermally treated at a desired temperature for 12 h under stirring conditions. After the second-step hydrothermal treatment, the product was filtered and washed with the distilled water, and then dried at room temperature.

Physical Analysis. The crystal structure of the sample was investigated using a powder X-ray diffractometer (Shimadzu, Model XRD-6100) with Cu Kα (λ = 0.15418 nm) radiation. The size and morphology of the particles were observed using field-emission scanning electron microscopy (FE-SEM) (Hitachi, Model S-900). Transmission electron microscopy (TEM) observation and selected-area electron diffraction (SAED) were performed on a JEOL Model JEM-3010 system at 300 kV, and the powder sample was supported on a microgrid. Energy-dispersive spectroscopy (EDS) (JEOL Model JED-2300T) was

dx.doi.org/10.1021/cm2015252 |Chem. Mater. 2011, 23, 3978–3986

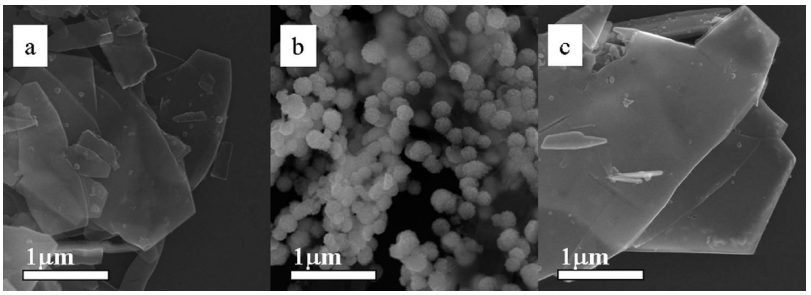

Figure 2. Field-emission scanning electron microscopy (FE-SEM) images of (a) the HTO precursor, (b) the BBKT sample obtained via hydrothermal treatment of HTO in $Ba(OH)_2$−$BiCl_3$−3-mol/L KOH water solution at 200 °C for 12 h, and (c) the BT−HTO nanocomposite sample.

measured on the TEM system. In the chemical composition analysis, the sample first was dissolved in a solution, and then the Ba, Bi, and Ti contents in the solution were measured using a sequential plasma spectrometer (Shimadzu, Model ICPS-7510) and K content in the solution was measured using an atomic absorption spectroscopy (AAS) system (Hitachi, Model AA78).

RESULTS AND DISCUSSION

Formation of $Ba_{0.5}(Bi_{0.5}K_{0.5})_{0.5}TiO_3$ under Hydrothermal Conditions. First, we investigate the formation reaction of $Ba_{0.5}(Bi_{0.5}K_{0.5})_{0.5}TiO_3$ (BBKT) phase from $H_{1.07}Ti_{1.73}O_4$ (HTO) under hydrothermal conditions. Figure 1 presents a phase diagram for the HTO−$Ba(OH)_2$−$BiCl_3$−KOH reaction system under the hydrothermal conditions. This phase diagram is obtained from XRD results of the products in the HTO−$Ba(OH)_2$−$BiCl_3$−KOH reaction system (see Figures S1 and S2 in the Supporting Information). At 150 °C, $BaTiO_3$ phase with a pseudo-cubic perovskite structure and a $Bi_{12}TiO_{20}$ phase (JCPDS File No. 34-0097) are formed mainly in a KOH concentration range of 0.5−1.5 mol/L, while single BBKT phase with the pseudo-cubic perovskite structure is formed mainly in a KOH concentration range of 3−8 mol/L. At 200 °C, the KOH concentration range of the BBKT phase formation expands to 0.5−8 mol/L.

The HTO precursor has a platelike particle morphology, with a particle size ~3 μm in width and 200 nm in thickness (see Figure 2a). After the hydrothermal reaction at 200 °C, spherical BBKT particles with a particles size of ~200 nm are obtained (Figure 2b), meaning the destruction of the precursor platelike morphology in the formation reaction of the BBKT phase. We find that the destruction of the platelike morphology occurs under all the reaction conditions where the single BBKT phase can be formed. This is due to the fact that a high KOH concentration and/or high reaction temperature are necessary for the formation of the BBKT phase, while the platelike morphology of HTO is very easy to be destroyed under these reaction conditions by a dissolution−deposition reaction. These results suggest that only the spherical particles of BBKT can be obtained by the direct hydrothermal treatment of HTO in the $Ba(OH)_2$−$BiCl_3$−KOH water solution, meaning that the spherical BBKT particles can be prepared by the conventional one-step hydrothermal process as described above, but not platelike BBKT particles.

Formation of $BaTiO_3$−HTO Nanocomposite Platelike Particles. To prepare BBKT platelike particles, we have developed a novel two-step solvothermal process to inhibit the platelike morphology destruction in the formation process of BBKT. In the first step, the HTO precursor is reacted partially with $Ba(OH)_2$ under the solvothermal conditions in a water−ethanol mixed solvent to obtain a $BaTiO_3$−HTO (BT−HTO) nanocomposite. In the second step, the BT−HTO nanocomposite is hydrothermally treated in $BiCl_3$−KOH water solution to transform it to the BBKT phase. Figure 3 presents the XRD patterns of samples obtained by the two-step solvothermal process. After the solvothermal treatment of HTO and $Ba(OH)_2$ (Ba/Ti molar ratio = 0.5/1) in the water−ethanol mixed solvent (volume ratio = 2:28) at 150 °C, a mixture of the HTO phase and a low crystalline $BaTiO_3$ (BT) phase are formed, indicating that the HTO precursor is partially transformed to BT phase.

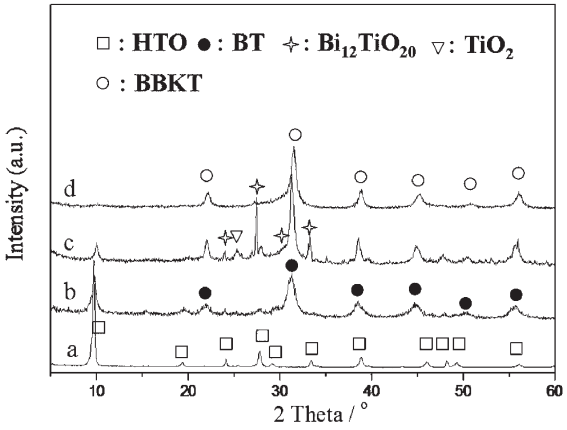

Figure 3. XRD patterns of (a) layered titanate HTO precursor, (b) BT−HTO nanocomposite, and samples obtained by hydrothermal treatment of BT-HTO nanocomposite in $BiCl_3$−3-mol/L KOH water solution at (c) 150 and (d) 200 °C for 12 h, respectively.

The FE-SEM result reveals that the BT-HTO nanocomposite sample retains the platelike morphology of the HTO precursor (see Figure 2c). Figure 4 shows the TEM images and SAED patterns of the HTO precursor and BT−HTO nanocomposite sample. The platelike HTO particle is a single crystal with a smooth particle surface. It is very interesting that the platelike particle of the BT−HTO nanocomposite is constructed from many small spherical nanoparticles with a particle size of ~10 nm. In the SAED pattern of the nanocomposite, two sets of SAED spots for the HTO layered phase and the BT perovskite phase are observed simultaneously in one platelike particle (see Figure 4d), indicating that BT and HTO phases coexist in one platelike particle. The spherical nanoparticles correspond to the BT phase, and these nanoparticles are inlaid into the platelike substrate

dx.doi.org/10.1021/cm2015252 |Chem. Mater. 2011, 23, 3978–3986

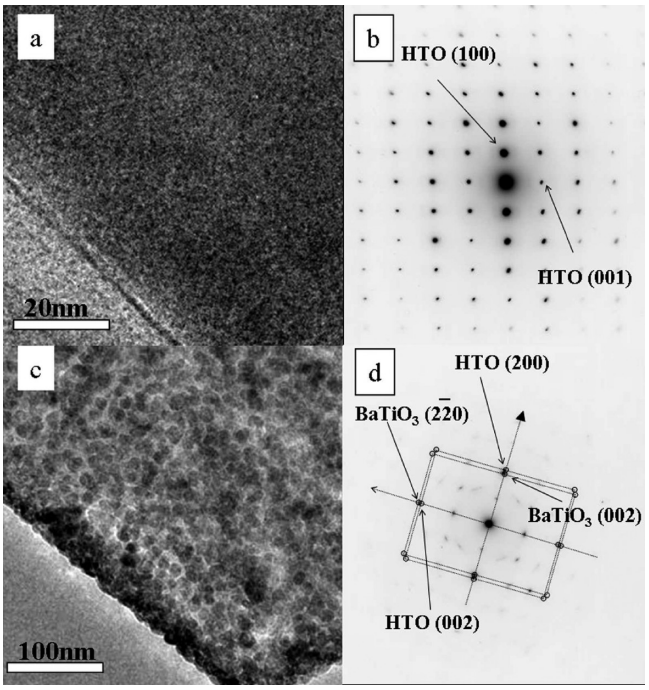

Figure 4. (a, c) TEM images and (b, d) SAED patterns of the HTO precursor (panels a and b) and BT−HTO nanocomposite (panels c and d) obtained by solvothermal treatment of HTO in $Ba(OH)_2$ solution.

of the HTO phase, forming the nanocomposite as shown in Figure 4c.

Transformation of $BaTiO_3$−HTO Nanocomposite into $Ba_{0.5}(Bi_{0.5}K_{0.5})_{0.5}TiO_3$ by Hydrothermal Reaction. In the second step, the BT−HTO platelike particles are hydrothermally treated in the $BiCl_3$−KOH solution to transform BT−HTO into the BBKT phase. After the hydrothermal reaction at 150 °C in a $BiCl_3$−3-mol/L KOH solution, the XRD peak intensity of the perovskite phase increases, but the unreacted HTO, and new phases of TiO_2 and $Bi_{12}TiO_{20}$ are observed also (Figure 3c), revealing that the formation reaction of BBKT is incomplete under these conditions. However, after the hydrothermal reaction at 200 °C in the $BiCl_3$−3-mol/L KOH solution, the unreacted HTO, TiO_2, and $Bi_{12}TiO_{20}$ phases disappear, and the single BBKT perovskite phase is obtained. The diffraction peaks of perovskite phase slightly shift to the larger 2θ valuess after the hydrothermal reaction, because the $BaTiO_3$ phase is transformed to the BBKT phase. The BBKT phase has the same pseudo-cubic perovskite structure as the $BaTiO_3$ phase, but has a slightly smaller lattice constant than the $BaTiO_3$ phase.[20] The $BaTiO_3$ phase in the BT−HTO nanocomposite sample has a lattice constant of a = 0.405 nm. After the transformation to the BBKT phase, the lattice constant decreases to 0.400 nm (see Figure 3d).

In order to understand the influence of KOH concentration on the formation of platelike BBKT particles in the $BiCl_3$−KOH solution, the reaction temperature and time are fixed to 200 °C and 12 h, respectively, and the KOH concentration is changed in a range of 0.1−8.0 mol/L. Figure 5 is the XRD patterns of samples obtained by the hydrothermal treatment of the BT−HTO nanocomposite at 200 °C. In the 0.1 mol/L KOH solution, except the perovskite phase, a $Bi_4Ti_3O_{12}$ phase (JCPDS File No. 47-0398) is formed. The diffraction peak intensity of the

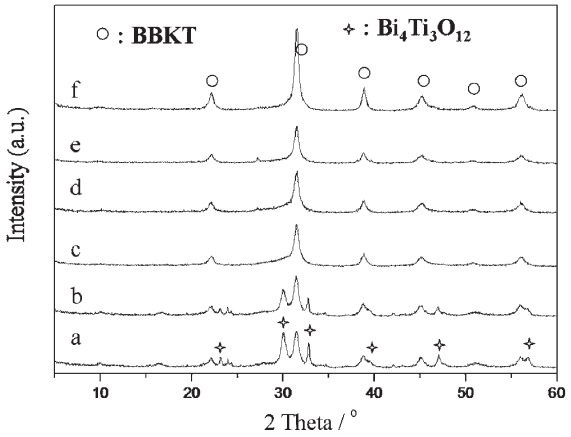

Figure 5. XRD patterns of sample obtained by the hydrothermal treatment of BT−HTO nanocomposite in $BiCl_3$−KOH water solution with different KOH concentrations at 200 °C for 12 h. The KOH concentrations are 0.1 mol/L (pattern a), 0.5 mol/L (pattern b), 1.5 mol/L (pattern c), 3.0 mol/L (pattern d), 5.0 mol/L (pattern e), and 8.0 mol/L (pattern f), respectively.

$Bi_4Ti_3O_{12}$ phase decreases with increasing KOH concentration, and then the $Bi_4Ti_3O_{12}$ phase disappears when the KOH concentration is higher than 1.5 mol/L, where only BBKT phase is observed. The diffraction peaks of the perovskite phase become sharper with increasing the KOH concentration. These results indicate that the single BBKT phase can be obtained when the KOH concentration is higher than 1.5 mol/L at 200 °C. Furthermore, its crystallinity increases with increasing KOH concentration. Chemical composition analysis result indicates that the molar ratio of Ba/Bi/K/Ti in the BBKT sample prepared in 8 mol/L KOH solution is 0.50:0.26:0.22:1, which is similar to the stoichiometric formation of $Ba_{0.5}(Bi_{0.5}K_{0.5})_{0.5}TiO_3$.

Figure 6 presents the FE-SEM images of the samples obtained by the hydrothermal treatment of BT−HTO in the $BiCl_3$−KOH solutions at 200 °C for 12 h. The samples retain the platelike morphology of the BT−HTO nanocomposite precursor after the hydrothermal reaction in a KOH concentration range of 0.1−8.0 mol/L. Each platelike particle is constructed from nanoparticles with a size of ~20 nm. In the KOH concentration range of 0.1−0.5 mol/L, sheetlike nanoparticles ~10 nm thick are observed on the surface of the platelike particles (see Figure 6a). The basal plane of the sheetlike crystals is always vertical to the basal plane of the platelike particle. The sheetlike crystals can be relegated to the $Bi_4Ti_3O_{12}$ phase, because the XRD result indicates the formation of $Bi_4Ti_3O_{12}$ in the KOH concentration range of 0.1−0.5 mol/L (see Figure 5), and also $Bi_4Ti_3O_{12}$ preferentially forms the sheetlike crystals.[30] The morphology of the nanoparticles in the platelike particle changes from irregular to cuboidlike as the KOH concentration increases from 0.5 mol/L to 8.0 mol/L (see Figure S3 in the Supporting Information), suggesting that the crystal growth occurs in the high KOH concentration solution. It is interesting that the cuboidlike nanoparticles regularly orient in platelike particle, suggesting the formation of a crystal-axis-oriented platelike BT−BKT particle. The above results reveal that the platelike BBKT particles can be prepared by the hydrothermal treatment of the BT−HTO nanocomposite.

Effect of Reaction Time on $Ba_{0.5}(Bi_{0.5}K_{0.5})_{0.5}TiO_3$ Formation. To study the formation mechanism of the platelike BBKT

dx.doi.org/10.1021/cm2015252 |Chem. Mater. 2011, 23, 3978–3986

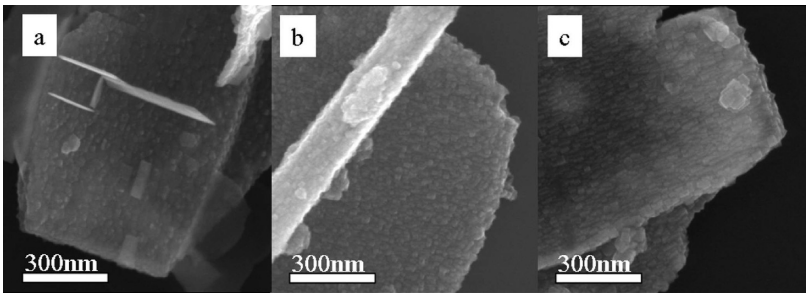

Figure 6. FE-SEM images of samples obtained by the hydrothermal treatment of the BT−HTO nanocomposite in a $BiCl_3$−KOH water solution with different KOH concentrations at 200 °C for 12 h; the KOH concentrations are (a) 0.5, (b) 3.0, and (c) 8.0 mol/L, respectively.

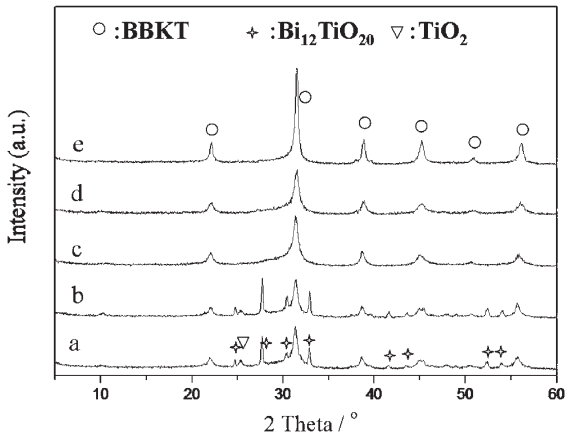

Figure 7. XRD patterns of samples obtained by hydrothermal treatment of the BT−HTO nanocomposite in $BiCl_3$−3-mol/L KOH water solution at 200 °C for 2 h (pattern a), 4 h (pattern b), 6 h (pattern c), 12 h (pattern d), and 48 h (pattern e).

particles, we investigate the effect of reaction time on the BBKT formation. Figure 7 presents the XRD patterns of samples prepared by the hydrothermal treatment of BT−HTO in the $BiCl_3$−3-mol/L KOH solution at 200 °C for different reaction times. The formations of $Bi_{12}TiO_{20}$ and TiO_2 are observed at 2 h. The $Bi_{12}TiO_{20}$ phase increases as the reaction time is prolonged up to 4 h, then decreases, and finally disappears after 6 h, forming the single BBKT phase. The crystallinity of BBKT becomes stronger as the reaction time is prolonged. These results indicate that the formation of the BBKT phase from the BT−HTO nanocomposite is a two-step reaction. In the first step, the $Bi_{12}TiO_{20}$ phase is formed by the reaction of the HTO phase in the nanocomposite with Bi^{3+} in the solution, or first the HTO phase is transformed into the TiO_2 phase, and then the TiO_2 phase reacts with Bi^{3+} in the solution to form the $Bi_{12}TiO_{20}$ phase. In the second-step, the BBKT phase is formed via reaction of the BT phase with the $Bi_{12}TiO_{20}$ phase in KOH solution.

The particle morphology change in the formation process from the BT−HTO nanocomposite to BBKT particles is investigated using FE-SEM (Figure 8). After the hydrothermal reaction for 4 h, hexahedron nanoparticles with a size of ∼50 nm are observed on the surface of the platelike particles, forming a platelike particle with a bumpy surface (see Figure S4 in the Supporting Information). The hexahedron nanoparticles on the platelike particle surface can be relegated to the $Bi_{12}TiO_{20}$ phase, because the XRD result indicates that the $Bi_{12}TiO_{20}$ phase is formed in the sample at the reaction time of 4 h (see Figure 7a). After the hydrothermal reaction for 6 h, the $Bi_{12}TiO_{20}$ nanoparticles disappear, and the surface of the platelike particles becomes smooth, forming platelike particles constructed from cuboidlike BBKT nanoparticles with a particle size of ∼30 nm (see Figure S4 in the Supporting Information). When the reaction time is prolonged to 48 h, the platelike particles tend to be split into the BBKT spherical nanoparticles with a particle size of ∼100 nm (see Figure 8c). The destruction of the platelike particle morphology is due to the crystal growth of BBKT nanoparticles in the platelike particle.

Nanostructural Study of Formation Reaction of $Ba_{0.5}(Bi_{0.5}K_{0.5})_{0.5}TiO_3$. Figure 9 presents the TEM images and EDS spectra for the BT−HTO nanocomposite and samples prepared via hydrothermal treatment of the BT−HTO nanocomposite in $BiCl_3$−3-mol/L KOH solution at 200 °C for different times. All these samples have the platelike particle morphology, and the platelike particles are the polycrystalline particles constructed from nanoparticles. The chemical composition distributions in these platelike particles are investigated using EDS analysis. Three positions (labeled as "A", "B", and "C" in Figure 9b) in each platelike particle of the BT−HTO nanocomposite present almost the same EDS spectra, suggesting a homogeneous chemical composition distribution in the platelike particle. Although the BT−HTO nanocomposite is the mixture of BT and HTO phases, the BT nanoparticles distribute uniformly in the platelike particle and the particle size of BT is very small (∼10 nm) (see Figure 4c). Since the detecting spot region of EDS is ∼10−15 nm, almost the same chemical composition is observed at different positions on the platelike particle. In the platelike particle of the BT−$Bi_{12}TiO_{20}$ mixed-phases sample prepared via the hydrothermal treatment of BT−HTO in $BiCl_3$−3-mol/L KOH solution at 200 °C for 4 h, the different positions (A, B, and C) present different EDC spectra; the Bi contents especially are quite different (see Figure 9d). In this sample, the surface of the platelike particle is covered by the $Bi_{12}TiO_{20}$ nanoparticles with relatively large size (∼50 nm), and the distribution of the $Bi_{12}TiO_{20}$ nanoparticles is not uniform (see Figure S4b in the Supporting Information). The BBKT platelike particle prepared via the hydrothermal treatment of BT−HTO in a $BiCl_3$−3-mol/L KOH solution at 200 °C for 12 h presents a uniform chemical composition distribution (see Figure 9f), meaning the homogeneous composition.

To investigate the structural transformation reaction mechanism from the HTO layered structure to the BBKT perovskite structure, a detail nanostructure analysis is performed on the BBKT platelike particles and its intermediate products in the

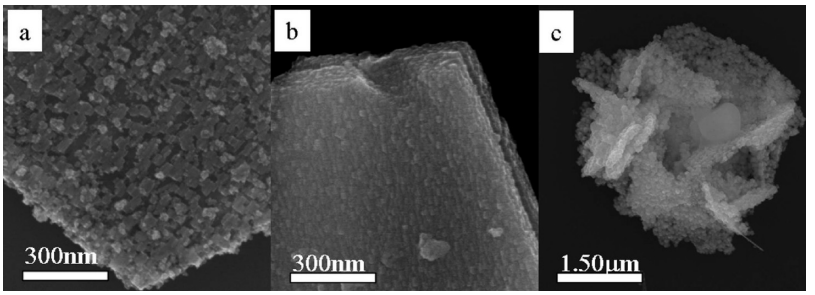

Figure 8. FE-SEM images of samples obtained by hydrothermal treatment of the BT−HTO nanocomposite in $BiCl_3$−3-mol/L KOH water solution at 200 °C for (a) 4, (b) 6, and (c) 48 h, respectively.

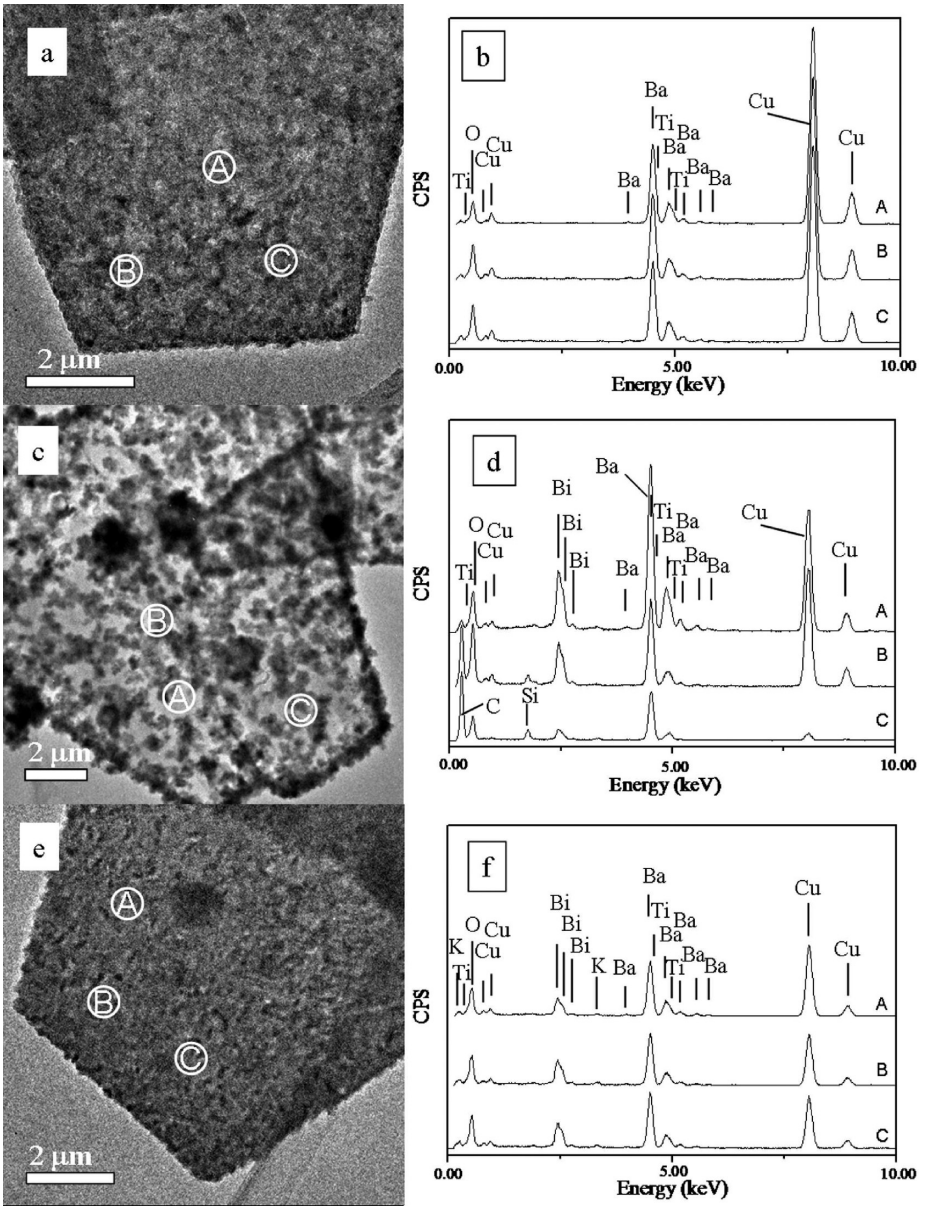

Figure 9. (a, c, e) TEM images and (b, d, f) EDS spectra of BT-HTO nanocomposite (panels a and b) and samples obtained by hydrothermal treatment of the BT−HTO nanocomposite in $BiCl_3$−3-mol/L KOH water solution at 200 °C for 4 h (panels c and d) and 12 h (panels e and f). EDS spectra of the regions labeled "A", "B", and "C" respectively correspond to those observed at the positions marked A, B, and C in TEM images.

transformation process using TEM and SAED. In the SAED pattern of the BT−HTO nanocomposite, two sets of diffraction spots are observed simultaneously (see Figure 4d). The diffraction spots with *d*-values of 0.376 and 0.285 nm correspond to the

dx.doi.org/10.1021/cm2015252 |*Chem. Mater.* 2011, 23, 3978–3986

(200) and (002) planes of the HTO layered structure, respectively. The diffraction spots with *d*-values of 0.198 and 0.141 nm correspond to the (002) and (2$\bar{2}$0) planes of the BT perovskite structure, respectively. We find a definite relationship between the crystal-axis directions of HTO and BT phases in one platelike particle of the BT−HTO nanocomposite. The *a*-axis direction of HTO layered structure corresponds to the *c*-axis direction of $BaTiO_3$ structure, and the *c*-axis direction of the layered structure corresponds to the [1$\bar{1}$0]-direction of $BaTiO_3$ structure. This result indicates that all the BT nanoparticles in one BT−HTO nanocomposite particle have the same orientation and the [110]-direction is vertical to the basal plane of the platelike particle.

Figure 10 presents the SAED patterns and HRTEM images of the BT−$Bi_{12}TiO_{20}$ sample and the BBKT sample obtained by the hydrothermal treatment of the BT−HTO nanocomposite sample for 4 and 12 h, respectively. The BT−$Bi_{12}TiO_{20}$ sample also presents two sets of diffraction spots in its SAED pattern. The diffraction spots with *d*-values of 0.163 and 0.258 nm correspond to the (620) and (004) planes of the $Bi_{12}TiO_{20}$ structure. Moreover, a clear lattice image of $Bi_{12}TiO_{20}$ structure with a lattice spacing of $d_{(220)}$ = 0.352 nm is observed in the HRTEM image. The diffraction spots with *d*-values of 0.399 and 0.285 nm correspond to the (001) and (1$\bar{1}$0) planes of the $BaTiO_3$ perovskite structure. This result indicates that there is a definite relationship between the crystal-axis directions of $Bi_{12}TiO_{20}$ and BT phases in one platelike BT−$Bi_{12}TiO_{20}$ particle. The *c*-axis direction of $Bi_{12}TiO_{20}$ structure corresponds to the *c*-axis direction of the BT structure, the [310]-direction of $Bi_{12}TiO_{20}$ structure corresponds to the [1$\bar{1}$0]-direction of the BT structure. These results suggest that all the $Bi_{12}TiO_{20}$ nanoparticles in the platelike particle have the same crystal-axis orientation, and the BT nanoparticles in the platelike particle retains the [110]-orientation.

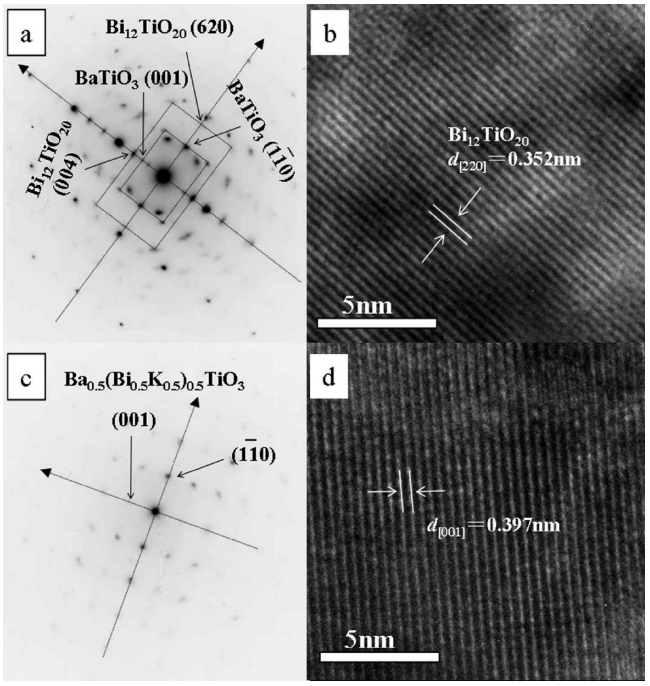

Figure 10. (a, c) SAED patterns and (b, d) HRTEM images of samples obtained by hydrothermal treatment of BT-HTO nanocomposite in a $BiCl_3$−3-mol/L KOH water solution at 200 °C for (a, b) 4 and (c, d) 12 h, respectively.

The BBKT sample presents one set of diffraction spots with *d*-values of 0.398 and 0.283 nm in the SAED pattern, similar to a single-crystal particle (Figure 10c). These diffraction spots correspond to the (001) and (1$\bar{1}$0) planes of a pseudo-cubic BBKT perovskite structure. In the HRTEM image, a lattice spacing of *d* = 0.397 nm can be assigned to the (001) planes of pseudo-cubic BBKT structure (Figure 10d). These results indicate that all the BBKT nanoparticles in one platelike particle have the same crystal-axis orientation, where the [110]-direction is vertical to the basal plane of the platelike particle, and this orientation is the same as that for BT nanoparticles in the platelike particle of the BT−HTO precursor. Therefore, the polycrystalline BBKT platelike particles with [110]-direction orientation are obtained by hydrothermal reaction of the BT−HTO platelike particles in $BiCl_3$−KOH solution. Such platelike BBKT particles will be very significant for the fabrication of oriented BBKT ceramic with small grain size, which is expected for high-performance piezoelectric materials, by applying domain engineering to oriented ceramics.

Formation Reaction Mechanism for $Ba_{0.5}(Bi_{0.5}K_{0.5})_{0.5}TiO_3$ Platelike Particles. A schematic representation of the formation mechanism of the BBKT platelike particle in the two-step solvothermal process is given in Figure 11. In the first step of the solvothermal treatment of HTO in a $Ba(OH)_2$ solution, first,

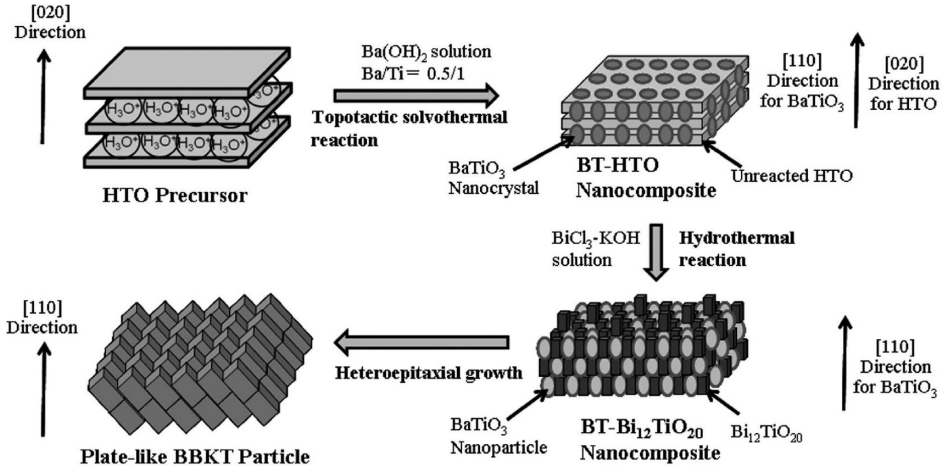

Figure 11. Formation mechanism of the platelike BBKT particle from HTO via a topotactic structural transformation reaction.

dx.doi.org/10.1021/cm2015252 |*Chem. Mater.* 2011, 23, 3978–3986

Ba^{2+} ions intercalate into the crystal bulk of HTO through the interlayer pathway by a H^+/Ba^{2+} exchange reaction, and then the Ba^{2+} ions react with the TiO_6 octahedral layers of HTO in the crystal bulk to form the BT phase via an in situ topotactic structural transformation reaction.[7] In the solvothermal reaction, half of the HTO is transformed to the BT phase, because the Ba/Ti mole ratio in the reaction system is 0.5/1. Since the topotactic structural transformation reaction occurs in the HTO crystal bulk, the uniform BT−HTO nanocomposite, as shown in Figure 4c, is formed, and the platelike particle morphology of the HTO precursor remains after the solvothermal reaction. Since the transformation reaction from HTO structure to BT structure is a topotactic reaction, there is a definite relationship between the structures of HTO and BT, indicating that there is a definite relationship between the crystal-axis directions of HTO and BT structures (see Figure 4d). Therefore, all the BT nanoparticles in one platelike particle of the BT−HTO nanocomposite have the same crystal-axis orientation in the [110]-direction.

In the second step of hydrothermal treatment of the BT−HTO nanocomposite in a $BiCl_3$−KOH solution, first, the $Bi_{12}TiO_{20}$ nanoparticles are formed on the surface of BT nanoparticles in the nanocomposite via the reaction of HTO and Bi(III). In this reaction, the HTO phase in the nanocomposite dissolves in the alkaline solution, reacts with Bi(III) in the solution, and then forms $Bi_{12}TiO_{20}$ on the surface of BT nanoparticles. Since the solubility of the $BaTiO_3$ phase is lower than the HTO phase in the alkaline solution, it almost does not take part in the formation reaction of $Bi_{12}TiO_{20}$, which keeps the BT-based platelike framework in the reaction. The SAED result indicates that all the $Bi_{12}TiO_{20}$ nanoparticles in the platelike particle show the same crystal-axis orientation (Figure 10a). This result suggests that the $Bi_{12}TiO_{20}$ nanocrystals grow on the surface of BT nanoparticles by a heteroepitaxial growth mechanism. In the heteroepitaxial growth process, the BT-based platelike framework acts as a porous substrate, where all the BT nanoparticles have the same crystal-axis orientation. In the final stage of the hydrothermal reaction, the BBKT phase is formed by the reaction of BT and $Bi_{12}TiO_{20}$ in KOH solution. This reaction is also a heteroepitaxial growth process with the BT-based platelike framework as the substrate, because all the BBKT nanoparticles in one platelike particle have the same crystal-axis orientation in the [110]-direction same as the BT nanoparticle. The mechanism described above suggests that the relatively low solubility of BT in the nanocomposite is important to keep the platelike particle morphology in the formation process of the BBKT phase.

CONCLUSIONS

The two-step solvothermal soft chemical process is an effective method for the preparation of the platelike $Ba_{0.5}(Bi_{0.5}K_{0.5})_{0.5}TiO_3$ (BBKT) particles. In the first solvothermal treatment step, the $BaTiO_3$−$H_{1.07}Ti_{1.73}O_4$ (BT−HTO) nanocomposite is formed by the partial transformation of HTO to BT. The formation reaction is the in situ topotactic structural transformation reaction. In the second hydrothermal treatment step, first, the BT−$Bi_{12}TiO_{20}$ nanocomposite is formed via reaction of the HTO phase in the BT−HTO nanocomposite with Bi^{3+} in the solution, and then the BBKT is formed by the reaction of the BT−$Bi_{12}TiO_{20}$ nanocomposite with KOH solution. The BBKT is formed by the heteroepitaxial growth on the BT-based platelike framework. The platelike BBKT particles prepared by this method are polycrystalline particles constructed from the nanocrystals, and the nanoparticles in each platelike particle show the same [110]-orientation.

ASSOCIATED CONTENT

Supporting Information. XRD patterns of the products in HTO−$Ba(OH)_2$−$BiCl_3$−KOH hydrothermal reaction system and FE-SEM images of the products in BT−HTO−$BiCl_3$−KOH hydrothermal reaction system. This material is available free of charge via the Internet at http://pubs.acs.org.

AUTHOR INFORMATION

Corresponding Author

*Tel.: +81(0)87-864-2402. Fax: +81(0)87-864-2402. E-mail: feng@eng.kagawa-u.ac.jp.

ACKNOWLEDGMENT

This work was supported in part by Grants-in-Aid for Scientific Research (B) (No. 23350101) from Japan Society for the Promotion of Science, and Kagawa University.

REFERENCES

(1) Feng, Q.; Hirasawa, M.; Yanagisawa, K. *Chem. Mater.* **2001**, *13*, 290.
(2) Feng, Q.; Honbu, C.; Yanagisawa, K.; Yamasaki, N. *Chem. Lett.* **1998**, 757.
(3) Feng, Q.; Honbu, C.; Yanagisawa, K.; Yamasaki, N. *Chem. Mater.* **1999**, *11*, 2444.
(4) Gopalakrishnan, J.; Uma, S.; Rangan, K. K.; Bhuvanesh, N. S. P. *Proc. Indian Acad. Sci.—Chem. Sci.* **1994**, *106*, 609.
(5) Komori, Y.; Sugahara, Y.; Kuroda, K. *Chem. Mater.* **1999**, *11*, 3.
(6) Sasaki, T.; Watanabe, M.; Fujiki, Y.; Kitami, Y. *Chem. Mater.* **1994**, *6*, 1749.
(7) Feng, Q.; Ishikawa, Y.; Makita, Y.; Yamamoto, Y. *J. Ceram. Soc. Jpn.* **2010**, *118*, 141.
(8) Wada, S.; Takeda, K.; Muraishi, T.; Kakemoto, H.; Tsurumi, T.; Kimura, T. *Jpn. J. Appl. Phys., Part 1* **2007**, *46*, 7039.
(9) Ge, H.; Hou, Y.; Wang, C.; Zhu, M.; Yan, H. *Jpn. J. Appl. Phys.* **2009**, *48*.
(10) Hiruma, Y.; Aoyagi, R.; Nagata, H.; Takenaka, T. *Jpn. J. Appl. Phys., Part 1* **2005**, *44*, 5040.
(11) Karaki, T.; Yan, K.; Miyamoto, T.; Adachi, M. *Jpn. J. Appl. Phys., Part 2: Lett.* **2007**, *46*.
(12) Reznitchenko, L. A.; Turik, A. V.; Kuznetsova, E. M.; Sakhnenko, V. P. *J. Phys. Condens. Mater.* **2001**, *13*, 3875.
(13) Wada, S.; Takeda, K.; Muraishi, T.; Kakemoto, H.; Tsurumi, T.; Kimura, T. *Ferroelectrics* **2008**, *373*, 11.
(14) Wada, S.; Kakemoto, H.; Tsurumi, T. *Mater. Trans.* **2004**, *45*, 178.
(15) Cao, W.; Randall, C. A. *J. Phys. Chem. Solids* **1996**, *57*, 1499.
(16) Kimura, T. *J. Ceram. Soc. Jpn* **2006**, *114*, 15.
(17) Fu, D.; Itoh, M.; Koshihara, S. Y.; Kosugi, T.; Tsuneyuki, S. *Phys. Rev. Lett.* **2008**, *100*.
(18) Buhret, C. F. *J. Chem. Phys.* **1962**, *36*, 798.
(19) Wada, T.; Fukui, A.; Matsuo, Y. *Jpn. J. Appl. Phys., Part 1* **2002**, *41*, 7025.
(20) Hiruma, Y.; Aoyagi, R.; Nagata, H.; Takenaka, T. *Jpn. J. Appl. Phys., Part 1* **2004**, *43*, 7556.
(21) Nagata, H.; Nemoto, M.; Hiruma, Y.; Takenaka, T. *Ceram. Trans.* **2010**, *221*, 55.
(22) Nemoto, M.; Hiruma, Y.; Nagata, H.; Takenaka, T. *Jpn. J. Appl. Phys.* **2008**, *47*, 3829.

(23) Nemoto, M.; Hiruma, Y.; Nagata, H.; Takenaka, T. *Jpn. J. Appl. Phys.* **2009**, 48.
(24) Tai, C. W.; Choy, S. H.; Chan, H. L. W. *J. Am. Ceram. Soc.* **2008**, *91*, 3335.
(25) Takeda, H.; Harinaka, H.; Shiosaki, T.; Zubair, M. A.; Leach, C.; Freer, R.; Hoshina, T.; Tsurumi, T. *J. Eur. Ceram. Soc.* **2010**, *30*, 555.
(26) Kimura, T.; Fukuchi, E.; Tani, T. *Jpn. J. Appl. Phys., Part 1* **2005**, *44*, 8055.
(27) Sugawara, T.; Nomura, Y.; Kimura, T.; Tani, T. *J. Ceram. Soc. Jpn.* **2001**, *109*, 897.
(28) Kong, X.; Ishikawa, Y.; Shinagawa, K.; Feng, Q. *J. Am. Ceram. Soc.* **2011**, in press (DOI: 10.1111/j.1551-2916.2011.04630.x).
(29) Feng, Q.; Hirasawa, M.; Kajiyoshi, K.; Yanagisawa, K. *J. Am. Ceram. Soc.* **2005**, *88*, 1415.
(30) Gu, H.; Hu, Z.; Hu, Y.; Yuan, Y.; You, J.; Zou, W. *Colloids Surf., A* **2008**, *315*, 294.